Bull. Chem. Soc. Ethiop. **2025**, 39(3), 483-502.
DOI: https://dx.doi.org/10.4314/bcse.v39i3.8

ISSN 1011-3924
Printed in Ethiopia
Online ISSN 1726-801X

ANTIBACTERIAL AND ANTIOXIDANT ACTIVITY OF PLANT-MEDIATED GREEN SYNTHESIZED SILVER NANOPARTICLES USING *Cissus quadrangularis* AQUEOUS EXTRACT

Ramesh Duraisamy, Abune Arizo and Belete Yilma*

Department of Chemistry, College of Natural and Computational Sciences,
Arba Minch University, Arba Minch, Ethiopia

(Received February 4, 2024; Revised December 3, 2024; Accepted December 4, 2024)

ABSTRACT. Plant-based green-synthesized silver nanoparticles (AgNPs) are valuable because of their advantages over traditional methods. This study examines the environment-friendly synthesized AgNPs using *Cissus quadrangularis* (CQ) stem aqueous extract. The optimum parameters for AgNP synthesis were a volume of plant extract (15 mL), aq. $AgNO_3$ concentration (0.10 mM), $AgNO_3$ volume (20 mL), reaction time (10 min), pH (11), and temperature (45 ºC). The synthesized AgNPs at optimum conditions were characterized through UV-Visible spectroscopy, FTIR, XRD, and SEM. In colloidal solutions, the occurrence of CQ-AgNP was studied through the color change measured by the UV-visible spectrum, which confirms the developed AgNPs with a typical resonance spectrum (at 430 nm). The percentage yield of synthesized AgNPs was also estimated as 94.32%. The FTIR spectra exhibit the availability of CQ phytochemicals responsible for the reduction, capping, and stabilization of Ag^+ of CQ-AgNP. The XRD pattern and SEM results show that the generation of highly crystalline spherical shapes of AgNPs has a mean diameter of 8.68 nm. Also, CQ-AgNPs had significant antibacterial activity against *S. aureus* and *E. coli*. The CQ-AgNPs had better antioxidant activity compared to the ascorbic acid standard. Thus, this study recommends that the presently studied CQ-AgNPs may be used as a remedial agent for biomedical applications.

KEY WORDS: Antibacterial, Antioxidant, *Cissus quadrangularis*, Green synthesis, Silver nanoparticles

INTRODUCTION

Nanoscience and nanotechnology have become increasingly important research areas in recent years. This research involves the creation of novel materials with sizes between 1 and 100 nanometers, a scale in which their physical and chemical properties can change dramatically [1], [2]. Nanoparticles can be synthesized using physical, chemical, or biological methods, each offering distinct benefits and challenges regarding particle size control, cost-effectiveness, particle distribution, and scalability. The versatility of these methods, along with the relatively low production costs and simplicity, makes AgNPs a highly favorable option for various applications [3]. The larger surface area and active sites on the surface of nanoparticles make them attractive to different applications, including catalysis, optics, electronics, and antibacterial activity [1, 4]. Various metal and metal oxide nanoparticles of Pd, Cu, Au, Zn, Sn, Ag, and Co have the potential for scavenging oxygen-based free radicals, making them candidates for new antioxidant therapies [4]. AgNPs generally comprise 20 to 15,000 silver atoms with diameters under 100 nm. Their large surface-area-to-volume ratio enhances their reactivity and efficiency in catalytic processes while providing potent antimicrobial effects, even at minimal concentrations [2]. Among them, silver nanoparticles (AgNPs) have momentous efficiency that is particularly promising for antibacterial-like biological applications because they control many bacteria, including *E. coli* and *S. aureus* [5]. AgNPs also have antioxidant properties, meaning they can help protect cells from damage by free radicals, which are unstable molecules that cause various diseases [5].

*Corresponding authors. E-mail: belete.yilma@amu.edu.et

Nanoparticles can be synthesized using different methods. The fastest and most efficient way to synthesize nanoparticles is by chemical processes, but they require toxic chemicals that pollute the environment. Physical methods do not use harmful chemicals but are more expensive and time-consuming than chemical methods [2, 4]. Additionally, traditional methods of synthesizing AgNPs are costly, toxic, and energy-intensive.

Medicinal plants, known for their rich content of essential phytochemicals long utilized in pharmaceutical applications, have gained increased attention [6]. Plant-based AgNPs, in particular, demonstrate promising antibacterial and anti-cancer activities, indicating their potential in various biomedical applications. In green synthesis, polyphenols and proteins naturally present in plants serve as efficient reducing agents, aiding in converting metal ions to lower oxidation states. Without strong ligands, metal ions interact with bioorganic reducing agents like flavonoids and terpenoids through ionic bonding. These organic compounds are added to a silver nitrate solution ($AgNO_3$ serving as the precursor) and act as capping and stabilizing agents, reducing Ag^+ ions to metallic Ag^0. Plants are readily available, and their various parts—such as roots, latex, stems, seeds, and leaves contain active components capable of reducing silver ions [4]. Compared to traditional chemical and physical methods, green synthesis offers several benefits, including non-toxicity, the absence of pollutants, environmental sustainability, cost efficiency, and ecological compatibility [2], [4].

AgNPs can be selectively functionalized with molecular capping agents, such as proteins and specific chemical groups, increasing their adaptability for targeted applications. Their exceptional antimicrobial properties have driven their use in antibacterial coatings, water purification systems, and wound dressings [7].

Recently, researchers focused on the synthesis of nanoparticles using a green approach, a relatively new method gaining popularity due to its environmental benefits. Plant-based green synthesis methods are economical and scalable, do not require higher temperatures, pressures, or toxic chemicals, and produce high-quality nanoparticles with a single-step approach [2]. It makes them a more sustainable and environmentally friendly way to synthesize nanoparticles. Additionally, plant extracts have abundant bioactive secondary metabolites, which could be used (as reducing and capping agents) to synthesize AgNP and stabilize them [8]. They are low-cost compared to microbial synthesize employing bacteria, fungi, algae, etc. [2]. The microbial-mediated process is quite costly and is complex due to the heresy of cultures [9].

Researchers are increasingly using plant extracts to make metal oxide nanoparticles. This "green" method involves mixing the extract with metal compounds under various conditions. The type and concentration of phytochemicals, the concentration of metals, pH, and temperature all affect the quality and quantity of the nanoparticles produced [2, 4]. In particular, plant extracts are better at reducing metal ions than bacteria or fungi, requiring less time.

Plant-based biological synthesis of nanoparticles is gaining attention due to its simplicity and eco-friendly nature. The reducing properties of various plant components play a crucial role in converting Ag^+ ions into AgNPs. The biosynthesis of AgNPs using different plant leaf extracts as bio-reducing, capping, and stabilizing agents has been widely studied [2, 4]. These reviews demonstrate that plant extracts are highly effective in generating silver nanoparticles. However, a thorough literature review reveals that there are only a few studies [10-13] focused on synthesizing silver nanoparticles using *Cissus quadrangularis* (CQ) stem extract as a plant-based reducing agent. Therefore, the present study used CQ stem extract to synthesize AgNPs and test their antibacterial and antioxidant activities.

Cissus quadrangularis is a perennial herb commonly found in tropical regions with notable medicinal properties. Rich in vitamin C and known for its antioxidant activity, this plant possesses various biomedical benefits, particularly its well-known anti-osteoporotic effects. Traditionally, it has been widely used in Ayurvedic medicine for treating conditions such as bone fractures, digestive issues, asthma, and weight management. Additionally, it is used in oral rehydration therapies, with each part of the plant serving distinct purposes [11]. CQ is traditionally used to

treat bacterial diseases, and AgNPs synthesized from CQ can be used as an alternative to reduce drug resistance. Antioxidants seize chain reactions by eliminating free radical intermediates and preventing other oxidation reactions from being oxidized.

Thus, this research aims to synthesize and characterize AgNPs through a plant-mediated green approach using CQ stem extract. The influence of the process (synthesis) conditions was studied; structural, morphological, and crystalline properties of AgNPs were also examined using Fourier transform infrared (FTIR) spectroscopy, scanning electron microscopy (SEM), and X-ray diffraction (XRD), respectively. The antioxidant activity (using a hydrogen peroxide assay) and antibacterial effectiveness of prepared AgNP against *Staphylococcus aureus* (gram-positive) and *Escherichia coli* (gram-negative) bacteria were also studied.

EXPERIMENTAL

Collection and identification of the stem of Cissus quadrangularis

Fresh stems of CQ were collected from Mulu Wongel village, Bere Kebele, Arba Minch city, Secha sub-city, Gambo zone, SNNPR, Ethiopia, and used to prepare aqueous extracts of CQ. The study area is 500 km from the southern part of the country. Geographically, the study area is located at a latitude of 6° 01′59″ N and longitude of 37° 32′59″ E, and the monthly mean temperature is above 18 ºC with an average elevation of 1269 meters above sea level.

Preparation of the stem extract of Cissus quadrangularis

Fresh and healthier CQ stems were collected and preserved in a plastic bag; the stem's surface was cleaned (with tap water and followed by double distilled water) to remove dusty debris. Fine pieces of the young stem (25 g) were boiled with demineralized water (100 mL), which was taken in a conical flask (500 mL). The extracted suspension was heated for one hour (at 80 °C) and filtered through Whatman No.1 filter paper. Then centrifuged (at 2000 rpm), the aqueous CQ stem filtrate was for 30 min; it was stored in the refrigerator (at 4 °C) until use as a multipurpose material (reducing, capping and stabilizing agent) to synthesize AgNPs [14, 15].

Phytochemical screening of CQ extract

The CQ aqueous extract (CQE) was analyzed their different phytochemicals of carbohydrates, phenolic compounds, alkaloids, flavonoids, tannins, terpenoids, saponins, glycosides, steroids, proteins using standard procedures reported earlier [8].

Synthesis of AgNP

Approximately 0.169 g of $AgNO_3$ (for a 1 mM solution) was dissolved in 1 litre of deionized water in an Erlenmeyer flask [1]. Stored the solution in a brown bottle in a dark room (to prevent it from decomposing in the presence of sunlight) until used to prepare silver nanoparticles [14].

For the synthesis of silver nanoparticles (AgNPs) under the green vegetal-mediated approach, CQ stem extract (100 mL) was added to one litre of $AgNO_3$ solution (1 mM). It was kept overnight at room temperature to facilitate reduction into Ag^+ ions [1]. The change in color from yellow to dark brown after five hours indicates that AgNPs had been synthesized. Then, the fully reduced solution was centrifuged (at 10,000 rpm) for 10 min, and the larger particles were removed. The supernatant solution was then re-dispersed in an aqueous medium and centrifuged further. A triplicate measurement was carried out to ensure the well-dispersion of AgNPs.

The liquid was poured off, and by using deionized water, the residue was washed and dried in a hot air oven. Residue was collected in a ceramic crucible and heated (at 400 ºC) in a furnace for

2 hours. Then, the Ag^+ was reduced to AgNP, which was monitored through the ultraviolet-visible spectral data at different intervals. The UV-Visible data were collected at 1 nm intervals by scanning the spectrum from 200 to 800 nm wavelengths. According to a previous study, the light white powder was dried in the air and kept for investigation [16].

Process conditions optimization for the synthesis of AgNP using CQE

Different factors, such as extract volume, $AgNO_3$ volume, temperature, time, pH, and silver ion concentration, were used to optimize AgNP synthesis. Generally, its physical properties (size, shape, and morphology) are mainly influenced by Ag^+ concentration, extract concentration, and reaction time. Bio-reduction of $AgNO_3$ was carried out under various conditions: heating time of CQ stems (10-30 min), concentration of $AgNO_3$ solution (0.05-0.15 mM), volume of aqueous extract of CQ stem (10-30 mL), volume of $AgNO_3$ solution (10-30 mL), temperature (30-50 ^oC) and pH (3-11). Each parameter was varied one at a time to examine its influence on the bio-reduction of Ag^+. Bio-reduction of Ag^+ was assessed at regular intervals by scanning the UV-Visible spectra (recorded in the range of 200 to 800 nm wavelength) of each sample.

Synthesized AgNP characterizations

Visualization

The color change in the solution provided initial evidence for the development of AgNP. The color change, which transitions from yellow to deep brown in an aqueous solution, stimulated the surface plasmon resonance (SPR) effect [1]. The persistence of the SPR band is a significant indicator that confirms the generation of AgNP. Moreover, this transition signifies the reduction of Ag^+ within the aqueous solution by utilizing the *Cissus quadrangularis* stem extract (CQE).

Determination of the percentage yield of green synthesized AgNP

The concentration of Ag^+ was measured using atomic absorption spectroscopy (AAS, Buck Scientific, 210 VGP FAAS, Germany). This technique explored the transition of Ag^+ to silver nanoparticles (AgNPs). After 24 h of allowing a mixture of aqueous CQE and a 1 mM $AgNO_3$ solution at pH = 11 to react, the mixture was centrifuged (at 5,000 rpm) for 15 min. According to a previous study, AgNP yield was calculated as a percentage [17].

$$\text{Total yield} = \frac{\text{Initial } [Ag^+] \text{ in ppm} - \text{Final } [Ag^+] \text{ in ppm}}{\text{Initial } [Ag^+] \text{ in ppm}} \times 100 \quad (1)$$

Analysis of CQ-AgNP using UV-visible spectroscopy

UV-Visible spectroscopic analysis (SCOROD-50, Germany) was used to detect the generation of CQ-AgNP. It is widely understood that the optical absorption patterns of AgNPs are primarily governed by SPR, which shifts toward a longer wavelength as the particle size grows. Furthermore, it is commonly recognized that their size and morphology influence primarily the absorbance of AgNP. Absorption measurements were taken across a spectrum from 200 to 800 nm, identifying a peak in absorbance at the highest point of the spectrum [18].

Fourier transforms infrared spectroscopic (FTIR) analysis

An FTIR study was performed to potentially recognize phytochemicals that reduce, capping, and stabilize the generation of CQ-AgNP [1]. Additionally, this technique aids in identifying the vibration patterns of functional groups within the AgNP synthesized using environmentally friendly methods. The CQ-AgNP was dried (at 45 ^oC) for 24 h to remove the volatile matter. Then, the thin sample pellets were prepared by mincing the CQ-AgNP with 10% KBr. The spectrum of

CQ-AgNP was recorded using FTIR spectroscopy (Shimadzu, Japan) over a range of wavelength: 4000-400 cm^{-1} [1].

Analysis of CQ-AgNP using XRD

The composition phases of CQ-AgNP, crystalline or amorphous nature, and texture or alignment were examined using an XRD analyzer (Shimadzu, XRD-7000, Japan). The CQ-AgNP was oven dried at 50 ^oC and examined. The diffraction patterns were obtained at 40 kV voltage and 30 mA current using CuKα radiation and determined the crystal structure of the prepared AgNP. Scanning was carried out in a range of 100 to 800 for 2θ angles at a speed of 2 degrees per minute. The data obtained from this process are used to calculate the interatomic spacing (d) using Bragg's equation: $n\lambda = 2d\sin\theta$ [19].

By comparing the diffraction pattern acquired from a sample and the established standard diffraction information (JCPDS), it becomes feasible to examine the crystal structure of currently prepared CQ-AgNPs in this study. The crystalline size domain is computed by assessing the width of the XRD peaks, employing the Debye-Schscherrer equation:

$$D = k\lambda / \beta \cos\theta \quad (2)$$

where: D - an average crystallite size domain; k - Scherer's constant geometric factor (0.9); λ - wavelength of X-ray source (0.1541 nm or 1.541 Å); β is diffraction peak FWHM; and θ is the angle of diffraction.

Scanning electron microscopy (SEM) analysis

SEM study describes the dimensions, configuration, and structure of prepared AgNPs. It involves directing a concentrated stream of high-energy electrons onto the surface of solid AgNP samples, generating various signals. The size and structure of the synthesized AgNPs were examined by SEM (JSM, 6390, Eindhoven, The Netherlands) at accelerating with 20 volts.

Antibacterial activity of CQ-AgNPs

To evaluate the antibacterial efficacy of AgNP, we chose gram-positive (*S. aureus*) and gram-negative (*E. coli*) bacteria. The inhibition of bacterial growth was examined (through an agar well-diffusion assay) through the diameter of the zone where growth was hindered [20]. Sterile Petri dishes were prepared by pouring Müller-Hinton agar and allowing it to solidify. Uniform swabbing of *S. aureus* and *E. coli* strains was performed on separate plates using sterilized cotton swabs. The holes in each plate were created using a sterilized stainless steel cork borer. The micropipettes introduced 50 µL of different AgNP concentrations (10, 15, 20, and 25 µg/mL) into each hole.

Incubated (at 37 °C) the Petri dishes with microorganisms and AgNPs for 24 h; using a ruler, measured the diameter of the inhibition zone on the underside of the inverted Petri dishes. Similarly, the agar well-diffusion assay method assessed the antibacterial effects of silver nitrate, chloramphenicol, aqueous CQE, and deionized water against microorganisms studied (*S. aureus* and *E. coli*). Each test was performed three times and documented the results as the mean diameter of the inhibition zone mean diameter ± SD [20, 21].

Antioxidant activity of CQ-AgNPs

The hydrogen peroxide neutralizing capacity of the prepared AgNP was examined by the procedure outlined in the literature [20, 22]. Different concentrations of AgNP (20-100 µg/mL) were prepared; 5 mL of each concentration sample solution combined with a previously prepared H_2O_2 solution (0.6 mL) with a PO_4^{3-} buffer (50 mM with pH: 7.4), which was used as a control

blank. At 230 nm, absorbance was measured after 10 min relative to a reference blank (ascorbic acid) using a UV-Visible spectrophotometer. Likewise, we examined the free radical scavenging activity using the aqueous CQE. The hydrogen peroxide scavenged (in %) by the test samples was calculated. The procedure was repeated thrice, and the results were documented as the average percentage of scavenging activity ± SD [20, 22].

Analysis and interpretation of data

Statistical analysis of the data obtained in this study was carried out using Origin Pro: 2018 (version 9.5; Origin Lab Corporation, Northampton, USA) and Image J software. Furthermore, techniques such as ultraviolet-visible, FTIR, XRD, and SEM were used to interpret the characteristics of the synthesized nanoparticles.

RESULTS AND DISCUSSION

Phytochemical screening of CQE

The phytochemical screening of freshly prepared CQE was evaluated by reviewing the availability of various phytoconstituents. The results presented in Table 1 confirm the existence of phenols, alkaloids, flavonoids, tannins, terpenoids, carbohydrates, saponins, glycosides, steroids, and proteins. Demonstrates the presence of polyphenols, which could act as reducing and stabilizing agents. A similar result had been reported in an earlier study [11]. These components are crucial in facilitating the reduction of Ag^+ ions to AgNPs. As the nitrates undergo oxidation and Ag^+ ions are reduced by CQE, the reaction mixture gradually changes color to reddish-brown (as shown in Figure 1), signifying the formation of silver nanoparticles [23].

Table 1. Phytochemical screening of the aqueous extract of the *Cissus quadrangularis* stem.

Phytochemical	Reagents used	Color intensity	Result
Phenols	Ferric chloride	Blue	+
Alkaloids	Marquis reagent	Dark orange	+
Flavonoids	Alkaline reagent test	Yellow fluorescence	+
Tannins	Gelatin test	White precipitation	+
Terpenoids	Chloroform and conc. H_2SO_4	Reddish brown	+
Carbohydrates	Molisch's reagent test	Dull violet	+
Saponins	Frothing test	Formation of copious lather	+
Glycosides	Glacial acetic acid and aq. $FeCl_3$	Generation of the brown ring at the interface	+
Steroids	Acetic anhydride	Violet to green	+
Proteins	Biuret test	Violet	+

Note: + sign for the present.

In plant extract-mediated synthesis, the bioreduction of Ag^+ ions to Ag^0 atoms involves electron transfer from biomolecules in the extract, as illustrated in Figure 1. Compounds such as polyphenols, saponins, flavonoids, terpenes, sugars, and alkaloids act as efficient reducing agents. These biomolecules donate electrons from functional groups like hydroxyl (-OH) and carboxyl (-COOH) to Ag^+ ions [2], facilitating their reduction to elemental silver (Ag^0).

When $AgNO_3$ dissolves in water, it dissociates into Ag^+ cations and NO_3^- anions. The negatively charged O^- in phenols or COO^- in organic acids forms electrostatic interactions with the positively charged Ag^+ ions. This interaction allows the transfer of electrons, reducing Ag^+ to Ag^0 [2], thereby generating silver nanoparticles (AgNPs), as depicted in the schematic diagram (Figure 1).

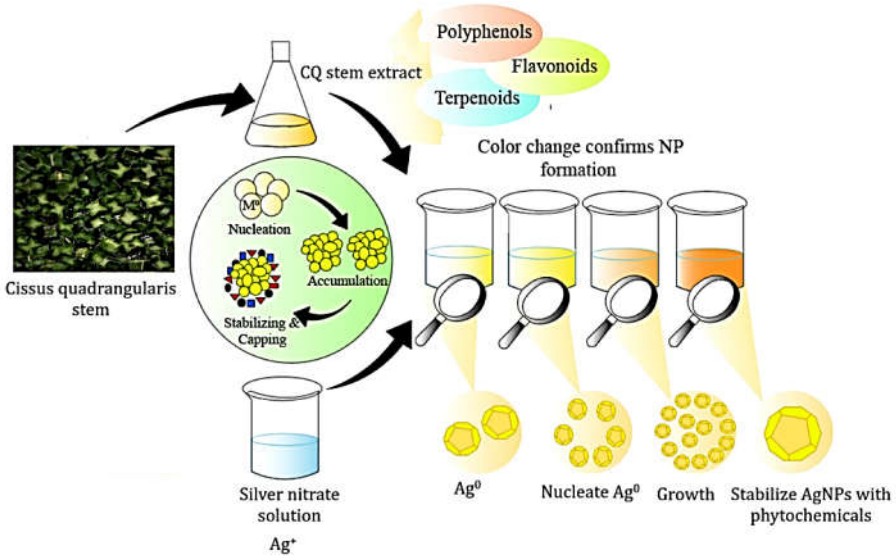

Figure 1. Mechanism of AgNPs synthesis using CQ stem extract adopted from the literature [24].

Process condition optimization for AgNPs synthesis using CQE

Optimizing the experimental parameters was crucial to attaining optimal conditions and enhancing the yield of silver nanoparticles (AgNPs). Various factors that impacted AgNP synthesis using CQE were fine-tuned. The variables subject to optimization included the extract volume, $AgNO_3$ concentration, duration of heating, pH, and processing temperature.

Effect of CQE volume

The synthesis of AgNPs was examined by introducing varying volumes of aqueous extract from CQ stems, ranging from 10 to 30 mL, into a silver nitrate solution. As shown in Figure 2a, the absorbance of AgNPs increased as the volume of CQ stem extract increased, reaching a peak at 15 mL. This indicates that achieving a complete reduction of Ag^+ ions in AgNPs requires a larger extract volume. On the contrary, higher extract concentrations (above 15 mL) decreased absorption, resulting in a cloudy solution. This phenomenon may be attributed to the excess availability of biomolecules in the CQE. Furthermore, when the CQE volume exceeds 15 mL, the absorbance of AgNPs decreases, possibly due to the increased binding capacity of phytoconstituents on the surface of AgNPs [25]. In the present study, the optimal CQE volume for AgNP synthesis was 15 mL, which was selected for subsequent trials.

Effect of $AgNO_3$ concentration

The influence of the substrate on the production of nanoparticles (NP) was investigated using various $AgNO_3$ concentrations (ranging from 0.05 to 0.15 mM) for the eco-friendly synthesis of AgNP. The study's results revealed that increasing $AgNO_3$ concentration up to 0.15 mM (shown in Figure 2b) facilitated the comprehensive reduction of Ag^+. This is evidenced by the fact that the absorbance also increases with an increase in $AgNO_3$ concentration from 0.05 to 0.1 mM. However, a subsequent rise in $AgNO_3$ concentration (0.15 mM) caused a decrease in absorbance

value and led to the change of the peak from surface plasmon resonance (SPR) to a longer wavelength (λ_{max} = 430 nm). This phenomenon was attributed to the aggregation and clustering of the synthesized CQ-AgNPs, resulting in their sedimentation.

The generation of CQ-AgNPs was discernibly less pronounced (with lower absorbance) at lower $AgNO_3$ concentrations, up to 0.1 mM (Figure 2b). Consequently, the optimal concentration for the process was 0.1 mM $AgNO_3$. This finding underscores how the Ag^+ concentration varies and impacts the morphology and size of the prepared CQ-AgNPs, which is supported by the earlier study [2, 26].

Effect of heating time

Exploring the impact of heating duration on AgNP synthesis, the extract, and $AgNO_3$ concentrations were kept constant while the heating time varied between 10 and 30 min. Incubation at room temperature (up to 24 h) was then recorded, UV-Visible spectra for the prepared material (CQ-AgNP) were recorded, and the results were illustrated in Figure 2c.

The degradation of phytochemicals in the presence of AgNP was evident through a consistent reduction in the intensity of the absorption peak at 430 nm, as depicted in Figure 2c. Notably, a significant observation was that a 10-minute heating period yielded the highest absorbance for the synthesized AgNPs. This absorbance gradually decreased with prolonged heating times, and longer heating times led to the deterioration of phytochemicals in the CQ stem, which reacted with the $AgNO_3$ solution. This reaction changed from yellow to dark brown within 10 min. These findings align with previous studies investigating similar phenomena [27].

Effect of pH

The impact of pH on AgNP preparation was investigated by altering the reaction mixture pH, ranging from 3 to 11. The noteworthy role of reaction pH lies in its ability to modify the electric charges on biomolecules, potentially influencing their ability to act as capping and stabilizing agents, thus impacting the growth of the nanoparticles. A minimal surface plasmon resonance (SPR) band was observed under low-pH conditions, which was attributed to generating maximum AgNPs.

The results of the current study suggest that alkaline pH is more favorable for the synthesis of AgNPs. The lack of AgNP formation at highly acidic pH levels could be attributed to the degradation or inactivation of bioactive molecules under such conditions. UV-Visible spectra (Figure 3a) revealed a decrease in absorbance intensity as the pH exceeded 5. Larger nanoparticles at elevated pH values could be attributed to unregulated aggregation due to the increased interaction of $AgNO_3$ ions (as shown in Figure 3a). In contrast, the intensified repulsion between ions as pH increases could hinder additional nucleation, forming smaller nanoparticles. The highest AgNP production was achieved at pH 11, evident from the color change compared to the color at the rest of the pH values, as shown in UV-Visible absorption spectra. This trend aligns with previous research showing that elevated pH levels promote the ability to reduce Ag^+ into AgNPs by facilitating electron transfer through abundant available reducing agents, leading to a rapid decrease in silver ions [2].

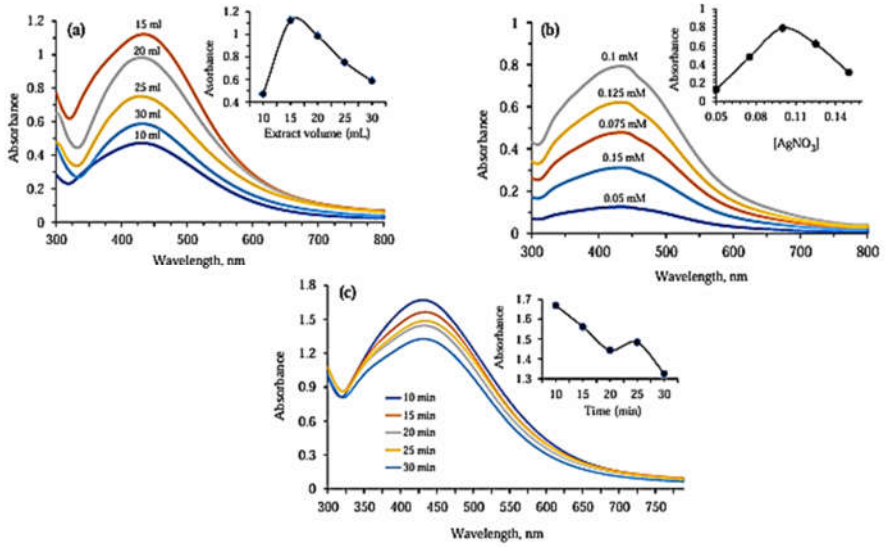

Figure 2. UV-Vis spectrum and the relation between the maximum absorption of synthesized AgNPs upon (a) different volumes of CQ stem aq. Extract, (b) different concentrations of $AgNO_3$ and (c) at different heating time.

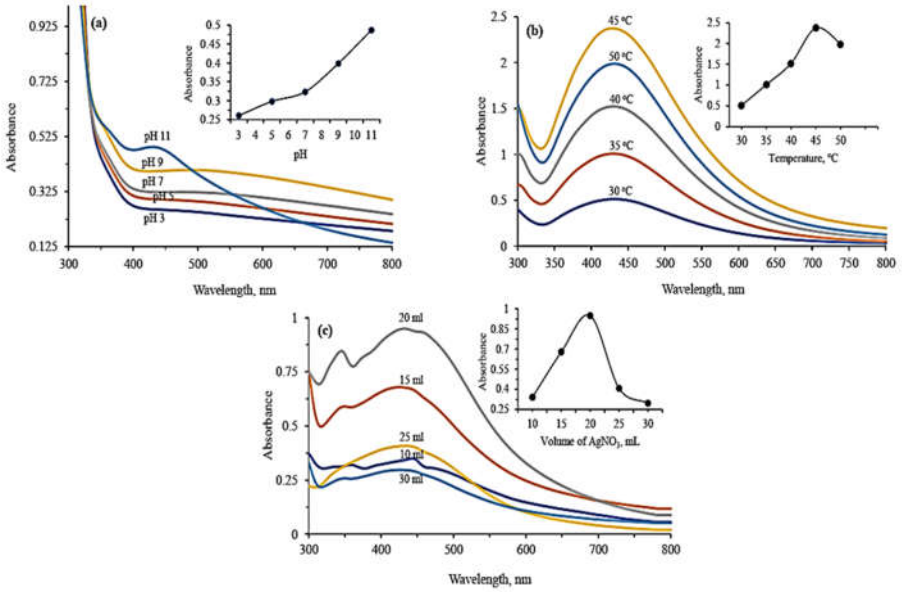

Figure 3. UV-Vis spectrum and the relation between maximum absorption of synthesized AgNPs and (a) pH, (b) different temperature and (c) volume of $AgNO_3$.

Effect of temperature

Examined CQ-AgNP production by temperature impact using a mixture of CQE (at pH 11) and 0.15 mM $AgNO_3$, which was incubated at various temperatures (ranged: 30-50 °C) in 5 °C intervals, as depicted in Figure 3b. Current study confirmed the dimensions of AgNPs decrease as the reaction temperature increases. The highest AgNP yield was observed at 45 °C and maintained stability over an extended period. Elevated temperatures contribute to higher kinetic energy, leading to an accelerated rate of synthesis [26], achieving the optimal yield of CQ-AgNPs at higher temperatures. It is supported by the literature, which suggests that increasing temperature intensifies the intensity of the SPR band due to a bathochromic shift, reducing the average diameter of AgNPs [26]. This is further supported by research using olive leaf extract to synthesize AgNPs [28]. The study found that raising the reaction temperature accelerated the reduction of Ag^+ ions and the nucleation of silver, resulting in the formation of tiny, spherical nanoparticles. Additionally, it was observed that *Vitex agnus-castus* leaf extract could rapidly reduce Ag^+ ions even at a relatively low temperature of 40 °C [28]. Thus, it is well established that even lower temperatures (studied optimized temperature: 45 °C) favor the growth of nanoparticles during synthesis. Higher temperatures can denature plant-derived biomolecules, while lower temperatures may slow the reduction process. At 45 °C, the biomolecules retain their reducing and capping activity, facilitating efficient nanoparticle synthesis while maintaining particle stability. Also, Temperatures around 45 °C are often ideal for ensuring a high nucleation rate without excessive particle growth.

Effect of the volume of silver nitrate

The impact of $AgNO_3$ volume on the synthesis of CQ-AgNPs was investigated, and the results obtained are presented in Figure 3c. At a volume of 20 mL of $AgNO_3$ solution, the highest absorbance was recorded, indicating that the whole Ag^+ reduces to AgNP. The absorption peaks at larger $AgNO_3$ volumes indicated that Ag^+ reduces to Ag° at a minor level and suggested the availability of AgNP with a broader size distribution [29]. The concentration of Ag^+ may increase, and the absorption peak becomes more distinct, exhibiting a maximum intensity at 430 nm. The spectra' surface plasmon resonance (SPR) peaks were most effectively manifested in the case of 20 mL of $AgNO_3$ solution.

Green synthesized CQ-AgNP characterizations

When the aqueous extract of CQ stems was introduced to the $AgNO_3$ solution, an observable color transfer was observed, signifying the creation of AgNP. The vegetal synthesized AgNPs were characterized using UV-Vis., FTIR, XRD, and SEM analyses. The AgNPs produced via the green synthesis technique were subjected to characterization processes that allowed the correlation of the color alteration in the reaction mixture with structural traits, crystal phases, surface features, chemical composition, and optical attributes visual transformation validated by reduction of Ag^+ ions. The structure of CQ-AgNPs and crystal phase were determined through XRD pattern analysis, while SEM analysis confirmed the prepared CQ-AgNP surface morphology.

Percentage yield of AgNPs using atomic absorption spectroscopy

Atomic absorption spectroscopy (AAS) was used to examine the concentration of unreacted metal ions in the reaction mixture (metal salt solution with plant extract), representing the change of metal ions into NPs [30]. Synthesized NPs were centrifuged at 10000 rpm for 10, 20, 30, and 40 min after 24 hours of incubation. The initial concentration of Ag^+ in the present study was obtained at 19.9 mg/L using AAS.

The decrease in the silver ion concentration from 2.19 to 1.13 mg/L reveals the settlement of AgNPs by centrifugation. The percentage yield of synthesized AgNPs increased with the enhancement of the centrifugation time by up to 30 min, beyond the 30-min centrifugation time, the percentage yield of AgNPs remained the same. Thus, the present study has a comparatively higher AgNP result (94.32%).

Visual observation

The alteration in the solution color provided initial evidence for the creation of CQ-AgNPs. The yellow to deep-brown color change in an aqueous medium (as shown in Figure 4) was the result of the stimulation of the surface plasma resonance effect (SPR) [2]. The persistence of the SPR band is a significant indicator affirming the generation of CQ-AgNP [17]. Moreover, this shift signifies the reduction of Ag^+ within the aqueous medium using CQE.

Figure 4. The color changes of the samples (a) yellow color of the aq. extract of the *Cissus quandragularis* stem aq. Extract, (b) $AgNO_3$ solution and (c) dark brown color of AgNP formation.

UV-Visible spectral study

Furthermore, confirmation of extracellular AgNP synthesis was achieved through UV-Visible spectroscopic analysis. The spectrum obtained revealed a prominent peak at 430 nm (Figure 5a), confirming the formation of AgNPs by reducing Ag^+ ions. Also, the present investigation suggests that the SPR pertained to nanoparticles below 100 nm. This observation aligns with previous findings and could be attributed to the activation of electrons within the conductive band near the AgNP surface [31]. Thus, the absorption peak at 430 nm indicates the reduction of Ag^+ to Ag^0 in the form of AgNPs in the solution mixture.

Stability test

They followed the optimization of the synthesis parameters and the stability of CQ-AgNPs. The prepared solution of AgNP was preserved at room temperature in the dark. Subsequently, the durability of the nanoparticles was assessed through UV-Visible spectral analysis, where the spectra were captured at varying intervals (1, 2, 3, 4, 5, and 6 months). Throughout this study, there was no noticeable alteration in color intensity, spectral peak placement, or AgNP absorbance when the sample was examined periodically over six months. AgNPs produced by green synthesis demonstrated a stable nature for this half-year period, maintaining their surface plasmon

absorbance band without any changes [32]. This outcome implies that the phytochemicals that persist in the CQ stem acted as effective reducing agents. The stability of AgNPs is of paramount importance, particularly in applications like medicine. Various selected factors were used to optimize for synthesis and are pivotal for achieving robust stability and optimal yield while controlling the particle size.

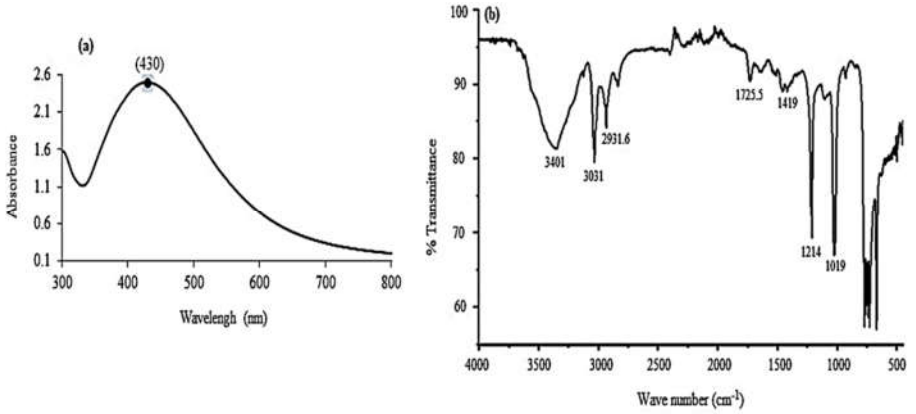

Figure 5. UV-Visible (a) and FTIR spectrum (b) of AgNPs synthesized at optimal conditions using *Cissus quandrangularis* stem aq. extract as a reducing and capping agent.

Analysis of CQ-AgNPs using FTIR

The FTIR study is utilized to identify potential functional groups of phytoconstituents present in CQE, which play a better role in nanoparticle (NP) synthesis. FTIR analysis makes it possible to determine whether the likely metabolites play a vital role in the reduction, capping, and adequate stabilization of AgNP and to understand the molecular environment of these capping agents on AgNP [2].

The FTIR spectrum of the prepared CQ-AgNPs confirmed that the plant extract had a dual function as a bio-reductant and a capping agent. In this analysis, great care was taken to prepare the sample to exclude any possibility of residual unbound CQE. AgNP generation after Ag^+ reduction, silver nitrate was admitted to centrifuge at 10000 rpm for 10 min. This step separated AgNP from any free biomolecules. The FTIR spectroscopy (Figure 5b) results of AgNPs synthesized through bioreduction are illustrated in Figure 4b. The FTIR spectrum displays absorption peaks at 3401, 3031, 2931.6, 1725.5, 1419, 1214, and 1019 cm^{-1} signifying the association of the available capping agent with the AgNP produced.

Absorption bands ranging from 3000 cm^{-1} to 3401 cm^{-1} correspond to the stretching vibrational frequency of the functional groups -OH and $-NH_2$ [13]. The peak at 2931.6 cm^{-1} originates from –CH stretching, associated with flavonoids. The intensive absorption at peak 1419 cm^{-1} corresponds to the bending of -OH in polyphenols, confirming the availability of aromatics. Furthermore, peaks at 1019 cm^{-1} are bonded ether (C-O-C) and the secondary -OH groups [2, 13]. The peak at 1725.5 cm^{-1} represents the carbonyl (C=O) functional group, which reduces Ag^+ to AgNPs. Also, the peak at 1214 cm^{-1} signifies C-N stretching vibration related to $-NH_2$ present in CQ-AgNP [2, 13].

These detected peaks provide validation that the NPs were enveloped by secondary metabolites from plants, including terpenoids, flavonoids, glycosides, phenols, and tannins. These metabolites incorporate different functional groups such as -CO, -CHO, -COOH, and others. The existence of these functional groups contributes to the stability of the CQ-AgNP. These secondary

metabolites play a vital role in preventing the aggregation and agglutination of nanoparticles, thus maintaining their dispersion.

X-Ray diffraction analysis of CQ-AgNPs

X-Ray diffraction (XRD) patterns have emerged as a valuable investigative technique, providing confirmation of AgNP formation, insight into the crystal structure of synthesized CQ-AgNP, and computation of particle size [4]. The crystalline nature of AgNPs synthesized via CQ stem extracts is verified using XRD spectra, and the corresponding XRD pattern is shown in Figure 6a.

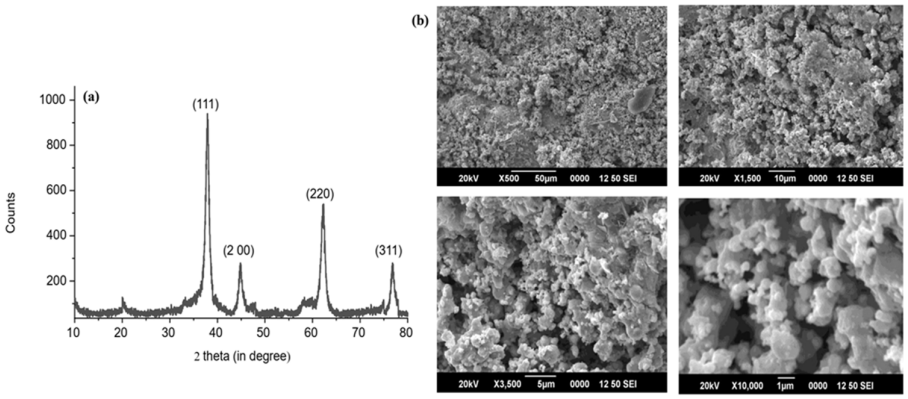

Figure 6. X-Ray diffraction pattern (a) and SEM image (b) with different magnifications of synthesized AgNPs using *Cissus quadrangularis* stem aq. extract.

The distinct diffraction peaks at 2θ values of 37.91°, 42.42°, 62.18°, and 78.04° are based on the respective crystallographic planes (111), (200), (220), and (311), respectively. In particular, the high-intensity peak is at 37.92º in plane (111), a sharper intensity of 100%. The crystallite sizes of the nanoparticle are calculated using the Debye-Scherrer formula. The average size of the crystalline, determined (using the Scherrer equation) by examined XRD peaks of the sample, is 8.68 nm.

This confirmed the crystalline structure of the CQ-AgNPs synthesized using the aqueous extract of *Cissus quadrangularis* stems. Similar findings have been reported, with higher crystalline particle sizes of 24 nm for AgNPs synthesized from *Cissus quadrangularis* extract and 70.89 ± 1.80 nm for those produced using *Cyclospermum leptophyllum* essential oil, respectively [12], [33].

Comparing the experimental diffraction pattern (2θ) of the synthesized AgNPs with standard diffraction angles is a form of fingerprint verification. The congruence between the powder diffraction patterns strongly supports the notion that the resulting particles are AgNPs. A comparison was made between the synthesized AgNPs and the standard silver nitrate reference provided by JCPDS (with File numbers 04-0783).

Morphological evaluation of CQ-AgNP using SEM

SEM images of the synthesized CQ-AgNP at varying magnifications: X500, X1500, X3500, and X10,000 are shown in Figure 6b. It reveals that the surface morphology of CQ-AgNPs produced through green synthesis is predominantly spherical. Additionally, the images demonstrate that the interactions and van der Waals forces between the AgNPs aggregate the nanoparticles. These aggregates manifest as particles with average dimensions ranging from 3 to 20 nm. The presently

studied CQ-AgNPs agreed well with the earlier literature, which used leaf extracts as a reducing and stabilizing agent and prepared the spherical AgNPs. The size range of these NPs was reported to range from 3 to 20 nm; this investigated result supported the previous studies about the green synthesis of AgNPs described in the literature [2], [4].

The particle size distributions of the currently prepared nanoparticles (NP) were evaluated using ImageJ software, employing a spherical approximation and calculated particle size based on deduced areas between 3 and 20 nm. SEM analysis was also utilized to assess the surface morphology and dimensions of AgNPs. The SEM image (Figure 6b) showed both individual AgNPs and aggregates. This depiction highlights the particles' prevalent spherical nature and tendency to form larger aggregates, a phenomenon mainly influenced by CQE secondary metabolites. Thus, SEM images of the CQ-AgNP indicated that the prepared AgNP is predominantly well-dispersed and spherical [12].

Antibacterial activity of AgNPs

The efficacy of the antibacterial activity of the studied CQ-AgNP against *S. aureus* and *E. coli* was evaluated using the agar well-diffusion technique. The results obtained are presented in Table 2.

Table 2. Inhibition zone (mm) of AgNP, aq. $AgNO_3$, chloramphenicol, aqueous extract of CQ stems at different concentrations, and deionized water.

Conc.	AgNP		Chloramphenicol		Aq. $AgNO_3$		*CQE*	
(µg/mL)	*S.aureus*	*E.coli*	*S.aureus*	*E. coli*	*S.aureus*	*E. coli*	*S.aureus*	*E. coli*
200	16 ± 0.29^{d}	13 ± 0.50^{d}	15 ± 0.43^{d}	12 ± 0.47^{d}	10 ± 0.44^{d}	8 ± 0.37^{d}	9 ± 0.76^{d}	7 ± 0.19^{d}
400	17 ± 0.61^{c}	15 ± 0.83^{c}	16 ± 0.45^{c}	13 ± 0.50^{c}	11 ± 0.66^{c}	10 ± 0.63^{c}	10 ± 0.85^{c}	8 ± 0.35^{c}
600	19 ± 0.83^{b}	16 ± 0.44^{b}	17 ± 0.37^{b}	14 ± 0.45^{b}	15 ± 0.76^{b}	12 ± 0.50^{b}	14 ± 0.66^{b}	10 ± 0.34^{b}
800	26 ± 0.54^{a}	17 ± 0.14^{a}	24 ± 0.66^{a}	15 ± 0.43^{a}	18 ± 0.29^{a}	14 ± 0.20^{a}	17 ± 0.19^{a}	11 ± 0.37^{a}

Note: The experimental results were expressed as mean±SD; different alphabets of superscripts in the column indicate the significant difference ($p \leq 0.05$) with a 95% confidence limit.

The effectiveness of different samples, including AgNP, $AgNO_3$, chloramphenicol, the aqueous extract of CQ stems, and Deionized water, was measured by quantifying the inhibition zone (at 37 °C) in bacterial growth after 24 hours of incubation. In particular, clear zones of gram-positive (*S. aureus*) and gram-negative (*E. coli*) bacteria were evident around the wells in all of the plates (shown in Figure 7). The appearance of these zones indicates that the test samples curtailed the growth of the microorganisms, and the size of the zones was determined by measuring their diameters.

As seen in the results in Table 2, the synthesized spherical shape with an average particle size of 8.58 nm of CQ-AgNPs displayed efficient antibacterial activity against both gram-positive and gram-negative bacteria. The silver nanoparticles synthesized using *Cissus quadrangularis* leaf aqueous extracts (800 µg/mL) showed the maximum zone of inhibition (26 ± 0.54 mm) for *S. aureus*, which were followed by *E. coli* (24 ± 0.66 mm). It is slightly higher than the chloramphenicol, aq. $AgNO_3$, and CQE alone.

Interestingly, an 800 µg/mL concentration of CQ-AgNP exhibits notably maximum antibacterial effectiveness, resulting in the largest inhibition zone diameter of 26 ± 0.54 mm against Staphylococcus aureus (Table 2). This value surpasses chloramphenicol, $AgNO_3$, and the CQ stem extract. This outcome can be elucidated by drawing a connection between the average size of AgNPs observed at 800 µg/mL, which showed a smaller size disparity. On the contrary, the other samples exhibited variations in size, encompassing larger particles or aggregates.

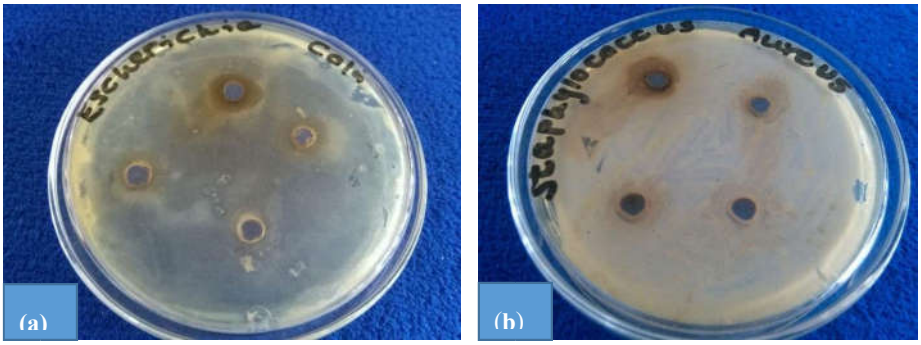

Figure 7. Zone of inhibition images of AgNPs (800 µg/mL) against (a) *E. coli* and (b) *S. aureus*.

Rota *et al.* [34] proposed a classification for antibacterial activity based on the zone of inhibition (ZoI), where weak activity is indicated by a ZoI ≤ 12 mm, moderate activity by a ZoI between > 12 and < 20 mm, and robust activity by a ZoI ≥ 20 mm. In this study, the CQ-AgNPs (with a size of 8.58 nm) exhibited potent antibacterial activity, particularly against Gram-positive bacteria, as evidenced by a larger ZoI (with 26 ± 0.54 mm, shown in Table 2). This enhanced activity is likely due to the antibiotic action of CQ-AgNPs, which disrupts peptidoglycan, a significant component of the Gram-positive bacterial cell wall. CQ-AgNPs bind to the terminal carboxyl group of D-alanyl-D-alanine in the nascent peptidoglycan, inhibiting the formation of lipid II, a crucial "shuttle carrier" for peptidoglycan monomers, which is evident in earlier [35]. This interaction forms hydrogen bonds with the peptide backbone, blocking its processing [36]. In contrast, the outer membrane of Gram-negative bacteria makes their cell walls more impermeable to larger glycopeptides, resulting in weaker activity against them. On the other hand, the lack of an outer membrane and periplasm in Gram-positive bacteria allows CQ-AgNPs to more easily permeate their hydrophilic, porous cell wall structure, leading to more potent antibacterial effects [37].

Also, the smaller particle size of CQ-AgNPs imparts an enlarged surface area-to-volume ratio, rendering them better productive than their larger counterparts. This characteristic enhances their binding capacity to bacterial membranes or facilitates cell proximity, increasing antibacterial activity [38]. Additionally, the bactericidal activity of AgNPs is closely related to their size and solubility. Nanoparticles smaller than 10 nm are exceptionally efficient at penetrating bacterial cell walls, causing considerable cellular damage [20, 39]. The release of silver ions from these tiny particles further boosts their antimicrobial effectiveness, highlighting the potential of AgNPs in combating microbial infections. So, combining the small nanoparticle size, bioactive compounds from *Cissus quadrangularis*, ROS production, and effective silver ion release makes the AgNPs highly effective against *S. aureus*, showcasing their potential as a powerful antimicrobial agent. This supports the currently studied CQ-AgNPs, which have an excellent antibacterial effect since they have been reported to lower the average particle size of 8.68 nm by the effect of *Cissus quadrangularis* extract.

The optimal antibacterial performance of AgNPs under this specific condition (800 µg/mL) underscores the appropriateness of the parameters applied for the green synthesis of CQ-AgNPs. However, the noticeable disparity in the inhibition zone between $AgNO_3$, CQE, and green synthesized AgNPs at 800 µg/mL against *S. aureus* could be related to previous findings suggesting that electrochemically generated silver ions are superior antibacterial agents compared to dissolved silver compounds [22]. Moreover, *E. coli* has a marginal contrast in the inhibition zone, potentially attributed to negatively charged lipopolysaccharides, making gram-negative bacteria more resilient than their gram-positive counterparts [40].

In the context of the microorganisms studied, the sequence of decreasing inhibition zone sizes among the test samples was as follows: AgNPs > chloramphenicol > silver nitrate > aqueous extract of CQ stems. In particular, AgNPs showed remarkable efficacy against S. aureus, producing the most expansive inhibition zone measuring 26 mm in diameter. It is in good agreement with the previous study by Paszek et al. [41], who reported that the higher antibacterial potential of AgNPs could be attributed to the discharge of silver cations that serve as reservoirs of bactericidal agents.

The findings demonstrated the substantial effectiveness of AgNPs against these drug-resistant organisms, in contrast to the lack of activity noticed in the negative control. The use of distilled water served to assess the potential impact of the medium within the experimental solution on the growth of *S. aureus* and *E. coli* bacteria. Notably, the antibacterial efficiency was attributed to the extracts containing AgNPs, not the solvent. These results are consistent with previous research indicating that the tiny size of AgNPs enhances their ability to breach bacterial outer walls, infiltrate cells, disrupt the respiratory chain, and consequently inhibit cell respiration, leading to bacterial death [42].

In the context of the dimensions of the inhibition zone, the antibacterial efficiency of the green synthesized CQ-AgNP in the present investigation can be classified as showing robust inhibitory activity following the criteria outlined by Davis and Stout [43].

Antioxidant activity of AgNP using hydrogen peroxide radical scavenging efficacy

An antioxidant is a substance that, when shown in a lower concentration relative to the oxidizable substrate, significantly retards or inhibits substrate oxidation. The scavenging capacity of CQ-AgNPs against hydrogen peroxide radicals was assessed with ascorbic acid, which served as the reference standard for comparison. The efficacy of the aqueous extract of CQ stems, standard ascorbic acid, and AgNP was evaluated to inhibit the activity of hydrogen peroxide radicals, and the findings are given in Table 3.

The initial H_2O_2 absorbance (control) (at 230 nm) was measured as 0.650. Subsequent absorbance measurements were taken after 10 min, revealing a lowering of H_2O_2 peroxide absorbance at 230 nm due to the presence of the test samples. The evaluated test samples exhibited noteworthy antioxidant activity compared to the standard utilized. The experiment results are reported as mean absorbance or percentage inhibition values ± SD. Hydrogen peroxide scavenged (in %) by the test samples was calculated following the methodology outlined in the literature [22], [44], and the results were reported in Table 3.

$$H_2O_2 \text{ Scavenging effect } (\%) = \frac{1 - \text{absorbance of the sample}}{\text{the absorbance of the control}} x\ 100 \quad (3)$$

Table 3. Hydrogen peroxide scavenging activity of AgNPs, ascorbic acid, and aqueous extract of CQ stem extract at different concentrations.

Conc. (µg/mL)	Mean absorbance ± SD			% Inhibition		
	AgNPs	CQ extract	Ascorbic acid	AgNPs	CQ extract	Ascorbic acid
30	0.404±0.002 [a]	0.452±0.004 [a]	0.516±0.089 [a]	37.85±0.07[e]	30.46±0.06[e]	20.62±0.09[e]
40	0.376±0.001[b]	0.416±0.002[b]	0.475±0.062[b]	42.15±0.01[d]	36.00±0.08[d]	26.92±0.09[d]
50	0.345±0.001[c]	0.371±0.002[c]	0.428±0.049[c]	46.92±0.06[c]	42.92±0.07[c]	34.15±0.02[c]
75	0.258±0.001[d]	0.267±0.003[d]	0.337±0.028[d]	60.31±0.08[b]	58.92±0.09[b]	48.15±0.02[b]
100	0.149±0.001[e]	0.191±0.002[e]	0.253±0.011[e]	77.08±0.03 [a]	70.62±0.02 [a]	61.08±0.02 [a]

Note: Triplicate experimental results were expressed as mean ± SD; different alphabets of superscripts in the column indicate the significant difference ($p \leq 0.05$) with a 95% confidence limit.

In Table 3, a decrease in hydrogen peroxide absorbance at 230 nm is evident, which indicates that both ascorbic acids, the aqueous extract of CQ stems, and AgNPs can effectively eliminate

free radicals. The evaluation of the hydrogen peroxide scavenging activity of AgNPs reveals that the highest observed antioxidant efficacy is 77.08 ± 0.03% at 100 µg/mL. In comparison, in 30 µg/mL concentration, the lowest antioxidant activity (37.85 ± 0.07%) was recorded. In a similar vein, the H_2O_2 scavenging activity of CQE (as shown in Table 4) exhibits a maximum antioxidant activity of 70.62 ± 0.02% in 100 µg/mL and minimal antioxidant activity of 30.46 ± 0.06% in 30 µg/mL.

Within standard ascorbic acid (Table 3), the assessment of H_2O_2 scavenging activity reveals the highest antioxidant efficacy recorded at 61.08 ± 0.02% in 100 µg/mL concentration. In comparison, the lowest observed antioxidant activity is 20.62 ± 0.09% in 30 µg/mL. Notably, there is an incremental trend in radical scavenging activity after increasing the concentrations among the tested samples. The order of the descending percent of scavenging activity for the test samples can be declined as ascorbic acid < aqueous extract of CQ stems < AgNP.

Consequently, the present study's findings demonstrate that with an increase in AgNP concentration ranging from 30-100 µg/mL, a more pronounced enhancement in inhibition is observed, ranging from 37.92 ± 0.07% to 77.07 ± 0.03%. This trend signifies that a higher concentration of AgNP corresponds to an increased percentage of hydrogen peroxide radical inhibition. A similar observation is described in the literature [20], suggesting that the elevated percentage of free radical scavenging activity in AgNPs is due to its ability as a potent oxidant in conjunction with the capping agents on its surface.

Hydrogen peroxide (H_2O_2) has significant harmful potential as it can permeate biological membranes. Although H_2O_2 is not inherently reactive, its presence within cells can sometimes lead to hydroxyl radicals, leading to toxicity [44]. The ability of the extracts to eliminate H_2O_2 could be attributed to their phenolic content, which provides electrons to H_2O_2, thereby neutralizing it and transforming it into water [44]. The findings underscore that all the extracts tested exhibited robust scavenging activity toward H_2O_2, probably due to the presence of antioxidant compounds. The antioxidant constituents within the extracts serve as competent electron contributors, which may accelerate the conversion of hydrogen peroxide into water.

H_2O_2 is recognized as a significant contributor to cellular aging and can adversely affect various cellular energy generation systems [20, 45]. The concentration-dependent scavenging activities of H_2O_2 were exhibited by AgNP, the aqueous extract, and ascorbic acid, as shown in Table 3. Specifically, in 100 µg/mL, the H_2O_2 scavenging activities were determined: AgNPs at 77.08%, CQ aqueous extract at 70.62%, and ascorbic acid at 61.08%. AgNPs demonstrated a notably higher H_2O_2 scavenging activity than aqueous extract and ascorbic acid. The results strongly suggest that AgNPs hold exceptional potential in effectively scavenging reactive oxygen species (ROS), further positioning them as a promising biological foundation for antioxidant applications [2].

CONCLUSIONS

In the current study, silver nanoparticles (AgNPs) were efficiently produced using an aqueous extract derived from CQ stems, achieving synthesis within a shorter incubation time (10 minutes) yielded a remarkable amount of 94.32% of AgNPs. The FTIR analysis revealed the dual capacity of the aqueous CQE, functioning as both an Ag^+ reducer and a stabilizer for CQ-AgNPs. XRD pattern of AgNPs exhibited a face-centered cubic structure and an average particle size of 8.68 nm. SEM micrograph indicated the prevalence of spherical nanoparticles with an average particle size of 3-20 nm. Notably, the current investigation revealed that no modifications were observed in the peak position, and the absorbance of AgNPs was synthesized through the green approach, even after six months. This enduring stability underscores the robust strength of synthesized AgNPs. Furthermore, currently studied CQ-AgNPs (800 µg/mL) exhibited noteworthy antimicrobial efficacy with the inhibition zone of 26 ± 0.54 mm and 17 ± 0.14 mm against the bacterial strains *S. aureus* and *E. coli*, respectively. The scavenging of free radicals by AgNPs (with 77.08 ± 0.03% inhibition of H_2O_2 scavenging) surpassed the standard ascorbic acid. Thus,

this study introduces an environmentally friendly, cost-effective, and potential method to produce AgNPs from harmless and renewable aqueous extract derived from the stems of *Cissus quadrangularis*, which acts as a reducing agent and stabilizer. The study concluded that investigated CQE and CQ-AgNP (with a smaller particle size of 8.68 nm) exhibited potential antibacterial and antioxidant properties, underscoring the significant potential in pharmaceutical and biomedical applications.

ACKNOWLEDGMENT

The authors thank the College of Natural Sciences of Arba Minch University in SNNPR, Ethiopia, for generously providing laboratory facilities for this research project.

REFERENCES

1. Shashiraj, K.N.; Hugar, A.; Rudrappa, S.; Bhat, M.P.; Almansour, A.I.; Perumal, K.; Nayaka, S. Exploring the antimicrobial, anti-cancer, and apoptosis-inducing ability of biofabricated silver nanoparticles using *Lagerstroemia speciosa* flower buds against the human osteosarcoma (mg-63) cell line via flow cytometry. *Bioengg.* **2023**, 10, 821.
2. Mohd, F.; Adnan, S.; Nahid, N.; Afroz, J.; Tahir, A.B.; Afreen, I. Green synthesis of silver nanoparticles: A comprehensive review of methods, influencing factors, and applications. *JCIS Open* **2024**, 16, 100125.
3. Palithya, S.; Gaddam, S.A.; Kotakadi, V.S.; Penchalaneni, J.; Golla, N.; Krishna, S.B.N.; Naidu, C.V. Green synthesis of silver nanoparticles using flower extracts of *Aerva lanata* and their biomedical applications. *Part. Sci. Technol.* **2022**, 40, 84-96.
4. Sanjida Akhter, M.; Ataur Rahman, M.; Rezaul Karim, R.; Mahfuza, M.; Mahmuda, A.; Shamim, M.; Firoj M.; Tajuddin, S.M. A systematic review on green synthesis of silver nanoparticles using plants extract and their bio-medical applications. *Heliyon* **2024**, 10, 29766.
5. Khattak, U.; Ullah, R.; Khan, S.A.; Jan, S.A. Rauf, A.; Ramadan, M.F. Synthesis, characteristics and biological activities of silver nanoparticles from Euphorbia dracunculoides. *Eur. Asian J. Biosci.* **2019**, 13, 2249-2260.
6. Nirmala, C.; Bajwa, H.K.; Oinam, S. Bamboo mediated green synthesis of silver nanoparticles-A new approach towards utilization of an underutilized plant. *Adv. Bamboo Sci.* **2024**, 6, 100061.
7. Akter, S.; Huq, M. Biologically rapid synthesis of silver nanoparticles by *Sphingobium* sp. MAH-11 T and their antibacterial activity and mechanisms investigation against drug-resistant pathogenic microbes. *Artif. Cell Nanomed. Biotechnol.* **2020**, 48, 672-682.
8. Bhagat, M.; Anand, R.; Datt, R.; Gupta, V.; Arya, V. Green synthesis of silver nanoparticles using aqueous extract of *Rosabrunonii lindl* and their morphological, biological and photocatalytic characterizations. *J. Inorg. Organometal. Polym.* **2019**, 29, 1039-1047.
9. Saif, S.; Tahir, A.; Chen, Y. Green synthesis of iron nanoparticles and their environmental applications and implications. *Nanomater.* **2016**, 6, 209.
10. Akshada, K.; Amol, S.; Anup, P.; Dipak, M.; Trupti, D.; Yeligar, V.C.; Monali, S.; Akshay, K.; Ranjit, J. Preparation and characterization of silver nanoparticles using Cissus quadrangularis extract and its in-vitro anti-arthritic activity. *Biol. Forum - Int. J.* **2023**, 15, 665-668.
11. Sumera, N.; Lakshmi Bhavani, N. Synthesis, characterization and phytochemical analysis of silver nanoparticles from the stem of *Cissus quadrangularis* L. *J. Emer. Tech. Innov. Res.* **2014**, 9, 93-103.

12. Kanimozhi, S.; Durga, R.; Sabithasree, M.; Vimal Kumar, A.; Sofiavizhimalar, A.; Avinash, A.K.; Ramakrishnan, R.; Sathya, R.; Nur Izyan, W.A. Biogenic synthesis of silver nanoparticle using *Cissus quadrangularis* extract and its invitro study. *J. King Saud Univ. - Sci.* **2022**, 34, 101930.
13. Vanaja, M.; Gnanajobitha, G.; Kanniah, P.; Rajeshkumar, S.; Malarkodi, C.; Annadurai, G. Phytosynthesis of silver nanoparticles by *Cissus quadrangularis*: Influence of physicochemical factors. *J. Nanostruc. Chem.* **2013**, 3, 17.
14. Kumar, B.; Smita, K.; Cumbal, L.; Debut, A.; Camacho, J.; Hernández-Gallegos, E.; Gustavo, R. Synthesis and biological activity of silver nanoparticles using *Passiflora tripartita* fruit extracts. *Adv. Mater. Lett.* **2015**, 6, 127-132.
15. Bhat, M.; Chakraborty, B.; Raju, S.; Abdulrahman, A.I.; Natarajan, A.; Kotresha, D.; Pallavi, S.S.; Dhanyakumara, S.B.; Shashiraj, K.N.; Nayaka. S. Biogenic synthesis, characterization, and antimicrobial activity of *Ixora brachypoda* (DC) leaf extract mediated silver nanoparticles. *J. King Saud Univ. - Sci.* **2021**, 33, 101296.
16. Chung, I.M.; Park, I.; Seung-Hyun, K.; Thiruvengadam, M.; Rajakumar, G. Plant-mediated synthesis of silver nanoparticles: Their characteristic properties and therapeutic applications. *Nanoscale Res. Lett.* **2016**, 11, 40.
17. Pochapski, M.T.; Fosquiera, E.C.; Esmerino, L.A.; dos Santos, E.B.; Farago, P.V.; Santos, F.A.; Groppo, F.C. Phytochemical screening, antioxidant and antimicrobial activities of the crude leaves extract from *Ipomoea batatas* (L.) Lam. *Pharmacog. Magaz.* **2011**, 7, 165.
18. Basavaraja, S.; Balaji, SD; Lagashetty, A.; Rajasab, A.H.; Venkataraman, A. Extracellular biosynthesis of silver nanoparticles using the fungus *Fusarium semitectum*. *Mater. Res. Bull.* **2008**, 43, 1164-1170.
19. Sri Ranjani, S. Phytochemical study on medicinal plant *Sida cordifolia* Linn. *Int. J. Multidis. Res. Dev.* **2015**, 2, 216-220.
20. Natasha, A.; Mohib, S.; Samreen, S.; Hadia, R. Plant mediated synthesis of silver nanoparticles and their biological applications. *Bull. Chem. Soc. Ethiop.* **2018**, 32, 469-479.
21. Mohamed, K.Y.; Soliman, A.H.; Hashem, A.A.; Al-Askar, G.A.; Salem, S.S. Green synthesis of silver nanoparticles from *Bauhinia variegata* and their biological applications. *Green Proc. Syn.* **2024**, 13, 20240099.
22. Jorge, L. Mejía-Méndez.; Gildardo, S.; Mónica, C.; Yulianna, M.; Diego, E.N.; Daniel Lozada-Ramírez, L.; Horacio, B.; Edgar, R.L.; Eugenio, S. Green synthesis of silver nanoparticles with extracts from Kalanchoe fedtschenkoi: Characterization and bioactivities. *Biomolecules* **2024**, 14, 782.
23. Mansour, K.G. Synthesis and characterization of silver nanoparticles from *Cocos nucifera* L. male flowers: An investigation into their potent antibacterial and anti-cancer efficacy. *Bull. Chem. Soc. Ethiop.* **2024**, 38, 725-724.
24. Nehil, S.; Sushant, B.; Ashhar Khan, M.; Yashi, V.; Saurabh, K.T.; Muskan, S. Green synthesis of nanoparticles and their biomedical applications: A review. *ACS Appl. Nano Mate.* **2021**, 4, 11428-11457.
25. Parveen, M.; Ahmad, F.; Malla, A.M.; Azaz, S. Microwave-assisted green synthesis of silver nanoparticles from *Fraxinus excelsior* leaf extract and its antioxidant assay. *Appl. Nanosci.* **2016**, 6, 267-276.
26. Husseiny, S.M.; Salah, T.A.; Anter, H.A. Biosynthesis of size-controlled silver nanoparticles by *Fusarium oxysporum*, their antibacterial and antitumor activities, Beni-Suef University. *J. Basic Appl. Sci.* **2015**, 4, 225-231.
27. Khalil, M.M.H.; Eman, H.I.; Khaled, Z.E.; Doaa, M. Green synthesis of silver nanoparticles using olive leaf extract and its antibacterial activity. *Arab. J. Chem.* **2014**, 7, 1131-1139.
28. Stavinskaya, O.; Iryna, L.; Tetiana, F.; Marina, K. Effect of temperature on green synthesis of silver nanoparticles using *Virex agnus-castus* extract. *Chem. J. Moldova* **2019**, 14, 117-121.

29. Oluwaniyi, O.O.; Adegoke, H.I.; Adesuji, E.T.; Alabi, A.B.; Bodede, S.O.; Labulo, A.H.; Oseghale, C.O.; Biosynthesis of silver nanoparticles using aqueous leaf extract of *Thevetia peruviana* Juss and its antimicrobial activities. *Appl. Nanosci.* **2016**, 6, 903-912.
30. Bansal, A.; Kaur, K. Silver nanoparticles-green synthesis through medicinal plant extract and its antimicrobial prospects. *J. Biol. Nat.* **2020**, 11, 34-41.
31. Naqvi, S.T.Q.; Shah, Z.; Fatima, N.; Qadir, M.I.; Ali, A.; Muhammad, S.A. Characterization and biological studies of copper nanoparticles synthesized by *Aspergillus niger*. *J. Bionanosci.* **2017**, 11, 136-140.
32. Govindaraju, K.; Tamilselvan, S.; Kiruthiga, V.; Singaravelu, G. Biogenic silver nanoparticles by *Solanum torvum* and their promising antimicrobial activity. *J. Biopest.* **2010**, 3, 394.
33. Yilma, H.G.; Mesfin, G.T.; Samuel, A.K.; Fekade, B.T.; Archana, B.; Kundan Kumar, C.; Rakesh Kumar, B. Biogenic synthesis of silver nanoparticles using essential oil of aerial part of *Cyclospermum leptophyllum* and their application in colorimetric determination of metallic ions. *Bull. Chem. Soc. Ethiop.* **2024**, 38, 213-228.
34. Rota, M.C.; Herrera, A.; Martínez, R.M.; Sotomayor, J.A.; Jordán, M.J. Antimicrobial activity and chemical composition of *Thymus vulgaris*, *Thymus zygis* and *Thymus hyemalis* essential oils. *Food Cont.* **2008**, 19, 681-687.
35. Chugunov, A.; Pyrkova, D.; Nolde, D.; Polyansky, A.; Pentkovsky, V.; Efremov, R. Lipid-II forms potential "landing terrain" for lantibiotics in simulated bacterial membrane. *Sci. Rep.* **2013**, 3, 1678.
36. Cong, Y.; Yang, S.; Rao, X. Vancomycin resistant *Staphylococcus aureus* infections: A review of case updating and clinical features. *J. Adv. Res.* **2020**, 21, 169-176.
37. Lawrence, R.; Tripathi, P.; Jeyakumar, E. Isolation, purification and evaluation of antibacterial agents from *Aloe vera*. *Braz. J. Microbiol.* **2009**, 40, 906-915.
38. Anitha, E.S.; Jayanthi, S.; Ramalingam, C.; Banerjee, C. Control of size and antimicrobial activity of green synthesized silver nanoparticles. *Mater. Lett.* **2016**, 185, 526-529.
39. Jacob, J.M.; John, M.S.; Jacob, A.; Abitha, P.; Kumar, S.S.; Rajan, R.; Natarajan, S.; Pugazhendhi, A. Bactericidal coating of paper towels via sustainable biosynthesis of silver nanoparticles using *Ocimum sanctum* leaf extract. *Mater. Res. Express* **2019**, 6, 045401.
40. Hwang, I.S.; Hwang, J.H.; Choi, H.; Kim, K.J.; Lee, D.G. Synergistic effects between silver nanoparticles and antibiotics and the mechanisms involved. *J. Med. Microbiol.* **2012**, 61, 1719-1726.
41. Paszek, E.; Czyz, J.; Woźnicka, O.; Jakubiak, D.; Wojnarowicz, J.; Łojkowski, W.; Stępień, E. Zinc oxide nanoparticles impair the integrity of human umbilical vein endothelial cell monolayer in vitro. *J. Biomed. Nanotechnol.* **2012**, 8, 957-967.
42. Skandalis, N.; Dimopoulou, A.; Georgopoulou, A.; Gallios, N.; Papadopoulos, D.; Tsipas, D.; Chatzinikolaidou, M. The effect of silver nanoparticles size produced using plant extract from Arbutus unedoon their antibacterial efficacy. *Nanomater.* **2017**, 7, 178.
43. Davis, W.W.; Stout, T.R. Disc plate method of microbiological antibiotic assay: II. Novel procedure offering improved accuracy. *Appl. Microbiol.* **2017**, 22, 666.
44. Gülçin, I.; Huyut, Z.; Elmastaş, M.; Aboul-Enein, H.Y. Radical scavenging and antioxidant activity of tannic acid. *Arab. J. Chem.* **2010**, 3, 43-53.
45. Dinda, G.; Halder, D.; Mitra, A.; Pal, N.; Vázquez-Vázquez, C.; López-Quintela, M.A. Study of the antibacterial and catalytic activity of silver colloids synthesized using the fruit of *Sapindus mukorossi*. *New J. Chem.* **2017**, 41, 10703-10711.